Neuronal differentiation of human mesenchymal stem cells: changes in the expression of the Alzheimer's disease-related gene seladin-1

EXPERIMENTAL CELL RESEARCH 312 (2006) 2592–2604

available at www.sciencedirect.com

SCIENCE DIRECT®

www.elsevier.com/locate/yexcr

Research Article

Neuronal differentiation of human mesenchymal stem cells: Changes in the expression of the Alzheimer's disease-related gene *seladin-1*

Susanna Benvenuti[a], *Riccardo Saccardi*[b], *Paola Luciani*[a], *Serena Urbani*[b], *Cristiana Deledda*[a], *Ilaria Cellai*[a], *Fabio Francini*[c], *Roberta Squecco*[c], *Fabiana Rosati*[a], *Giovanna Danza*[a], *Stefania Gelmini*[d], *Isabell Greeve*[e], *Matteo Rossi*[a], *Roberto Maggi*[f], *Mario Serio*[a], *Alessandro Peri*[a,*]

[a]*Endocrine Unit, Department of Clinical Physiopathology, University of Florence, Center for Research, Transfer and High Education on Chronic, Inflammatory, Degenerative and Neoplastic Disorders for the Development of Novel Therapies (DENOThe), Viale Pieraccini, 6, 50139 Florence, Italy*
[b]*Department of Haematology, Ospedale di Careggi, Florence, Italy*
[c]*Department of Physiological Sciences, University of Florence, Florence, Italy*
[d]*Clinical Biochemistry Unit (S.G.), Department of Clinical Physiopathology, University of Florence, Center for Research, Transfer and High Education on Chronic, Inflammatory, Degenerative and Neoplastic Disorders for the Development of Novel Therapies" (DENOThe), Viale Pieraccini, 6, 50139 Florence, Italy*
[e]*Department of Neurology, Inselspital University Hospital, Bern, Switzerland*
[f]*Laboratory of Developmental Neuroendocrinology, Department of Endocrinology, Centre of Excellence on Neurodegenerative Diseases, University of Milan, Milan, Italy*

ARTICLE INFORMATION

Article Chronology:
Received 14 November 2005
Revised version received
19 April 2006
Accepted 27 April 2006
Available online 6 May 2006

Keywords:
Seladin-1
Alzheimer's disease
Human mesenchymal stem cells
Neurons

ABSTRACT

Seladin-1 (SELective Alzheimer's Disease INdicator-1) is an anti-apoptotic gene, which is down-regulated in brain regions affected by Alzheimer's disease (AD). In addition, seladin-1 catalyzes the conversion of desmosterol into cholesterol. Disruption of cholesterol homeostasis in neurons may increase cell susceptibility to toxic agents. Because the hippocampus and the subventricular zone, which are affected in AD, are the unique regions containing stem cells with neurogenic potential in the adult brain, it might be hypothesized that this multipotent cell compartment is the predominant source of seladin-1 in normal brain. In the present study, we isolated and characterized human mesenchymal stem cells (hMSC) as a model of cells with the ability to differentiate into neurons. hMSC were then differentiated toward a neuronal phenotype (hMSC-n). These cells were thoroughly characterized and proved to be neurons, as assessed by molecular and electrophysiological evaluation. Seladin-1 expression was determined and found to be significantly reduced in hMSC-n compared to undifferentiated cells. Accordingly, the total content of cholesterol was decreased after differentiation. These original results demonstrate for the first time that seladin-1 is abundantly expressed by stem cells and appear to suggest that reduced expression in AD might be due to an altered pool of multipotent cells.

* *Corresponding author.*
E-mail address: a.peri@dfc.unifi.it (A. Peri).

0014-4827/$ – see front matter © 2006 Elsevier Inc. All rights reserved.
doi:10.1016/j.yexcr.2006.04.016

Introduction

A few years ago, a novel gene, named *seladin-1* (for SELective Alzheimer's Disease INdicator-1), was identified and associated to neurodegeneration. In fact, this gene was found to be down-regulated in brain regions affected by Alzheimer's disease (AD) [1]. Conversely, overexpression of seladin-1 conferred protection against β-amyloid-mediated toxicity and from oxidative stress in neuroglioma H4 cells. In addition, seladin-1 effectively inhibited caspase 3 activity, a key mediator of apoptosis, and protected from apoptotic death [1]. Accordingly, we have recently demonstrated in long-term cell cultures from human fetal olfactory epithelium that seladin-1, which is up-regulated by estrogen and Selective Estrogen Receptor Modulators, confers resistance to both β-amyloid-induced toxicity and oxidative stress [2]. Following its first description, a subsequent study demonstrated that seladin-1 possesses also enzymatic activity because its gene sequence was found to be identical to that of the gene encoding 3-beta-hydroxysterol delta-24-reductase (DHCR24) [3], which converts desmosterol into cholesterol. Disruption of cholesterol homeostasis may be detrimental for cells because a cholesterol-depleted membrane would ease the interaction with toxic factors such as β-amyloid [4]. With regard to its enzymatic activity, seladin-1 has been regarded as the human homologue of the *Diminuto/Dwarf1* gene, which is required in plants for the synthesis of brassinosteroids, a class of sterols essential for normal growth and development [5,6]. In humans, mutations of the *seladin-1* gene have been found in desmosterolosis, a rare severe multiple-congenital-anomaly syndrome, including developmental and growth retardation [3].

The hippocampus and the subventricular zone are two of the brain areas affected in AD [7]. Interestingly, these are the unique regions in which stem cells with a defined neurogenic potential are located in the adult brain [8]. In fact, although neural stem cells are present in many other areas of the adult brain, they do not appear to maintain the ability to differentiate into neurons [8]. Very recently, stem cells with neurogenic activity have been described also in the adult spinal cord [9,10], which classically was not considered a neurogenic region [11]. Noteworthy, Greeve et al. [1] detected the presence of rather high levels of expression of seladin-1 both in human normal hippocampus and spinal cord [1]. We hypothesized that, if seladin-1 expression is reduced in AD, stem cells might be the prevalent source of this protein. In order to test this hypothesis, we used mesenchymal stem cells (MSC), which have been reported to differentiate into different cell types in addition to mesenchymal derivatives, including neurons [12–15]. Admittedly, in our experimental design, this cell model might represent a reasonable alternative to the use of neuronal stem cells, which are much more difficult to obtain. In our hands, human MSC, obtained from aspirates taken from the iliac crest of normal young volunteers, were subjected to neuronal differentiation and both seladin-1 expression and the content of total cholesterol were determined in both undifferentiated and differentiated cells.

Materials and methods

Materials

Media and sera for cell cultures were purchased from Euroclone (Wetherby, West York, UK), and tissue plasticware was obtained from GreinerBio-One (Frickenhausen, Germany). Neurobasal medium was obtained from Life Technologies (Invitrogen, S. Giuliano Milanese, Milan, Italy). Other reagents for cell cultures were obtained from Sigma (Milan, Italy). Ultroser-G (UG) was purchased from Pall BioSepra SA (Cergy Saint Christophe, France). Flow cytometry buffer (CellWASH) was from Becton Dickinson (Franklin Lakes, NJ). Monoclonal antibodies for flow cytometry immunophenotyping were obtained from BD Pharmingen (San Diego, CA) and Ancell (St.N. Bayport, MN), whereas antibodies for immunocytochemistry were from Chemicon (Temecula, CA). For RNA extraction, the Nucleospin®RNAII kit was purchased from Macherey-Nagel (Duren, Germany). Reagents for RT-PCR studies were from Applied Biosystem Inc. (Foster City, CA). Cholesterol, Bradford reagent and *N*,*O*-bis(trimethylsilyl)-trifluoroacetamide (BSTFA) were from Sigma. Stigmasterol was from Steraloids Inc. (Newport, RI, USA). Pooled total RNAs from human adult tissues were from Clontech (Mountain View, CA).

Isolation, culture and characterization of human mesenchymal stem cells (hMSC)

Human bone marrow cells were obtained from the iliac crest of normal donors marrow aspirates. Informed consent was obtained from all donors, and the institutional ethical committee approved all the procedures. Whole bone marrow was collected, and small aliquots were centrifuged for 10 min at 700×*g*; the white blood cells buffy coat was recovered and plated in 75 cm^2 flasks (1.6×10^5 cells/cm^2) in Iscove's MDM (with L-glutamine and 25 mM HEPES) with 50 μg/ml gentamycin, 10% FBS and 2% UG. Cells were then incubated at 37°C in fully humidified atmosphere containing 95% air and 5% CO_2. On reaching confluence, the adherent cells were detached by 0.05% trypsin and 0.02% EDTA for 5–10 min at 37°C, harvested and washed with HBSS and 10% FBS and finally resuspended in complete medium (primary culture, P0). Cells were re-seeded at 10^4 cells/cm^2 in 100-mm dishes (P1) for both *in vitro* differentiation assessment and further cellular expansion which was achieved by successive cycles of trypsinization and re-seeding.

The frequency of Colony Forming Units-Fibroblasts (CFU-F) was measured using the method of Castro-Malaspina [16]. Visible colonies with 50 or more cells (the conventional value for defining a colony) [17] were counted and referred to 10^6 plated cells (no. of CFU-F/10^6 TNC).

Immunophenotyping and differentiation of hMSC

At the first passage, the morphologically homogeneous population of hMSC was analyzed for the expression of cell surface molecules using flow cytometry procedures: hMSC, recovered from flasks by trypsin–EDTA treatment and washed

in HBSS and 10% FBS, were resuspended in CellWASH buffer (0.1% sodium azide in PBS) with 2% FBS. Aliquots (1.5×10^5 cells/100 μl) were incubated with the following conjugated monoclonal antibodies: CD34-PE, CD45-FITC, CD14-PE (in order to quantify hemopoietic–monocytic contamination); CD29-PE, CD44-FITC, CD166-PE, CD90-PE, CD73-PE, HLA-DP QR-FITC, HLA-ABC-FITC (BD Pharmingen, San Diego, CA) and CD105-PE (Ancell, St.N. Bayport, MN). Non-specific fluorescence and morphologic parameters of the cells were determined by incubation of the same cell aliquot with isotype-matched mouse monoclonal antibodies. Incubations were performed for 20 min, and thereafter the cells were washed and resuspended in 100 μl of CellWASH; 7-AAD was added in order to exclude dead cells from the analysis. Flow cytometric acquisition was performed by collecting 10^4 events on a FACScan (argon laser equipped; Becton Dickinson) instrument, and data were analyzed on DOT-PLOT bi-parametric diagrams using CELL QUEST software (Becton Dickinson, Franklin Lakes, NJ, USA) on Macintosh PC.

The ability of MSC to differentiate along osteogenic, adipogenic and chondrogenic lineages was assayed, as described previously by Pittenger et al. [18]. Osteogenic, chondrogenic and adipogenic differentiation were evaluated by cytochemical analysis. Petri dishes were stained to assess glucosamynoglycans by Toluidine Blue and for extracellular matrix mineral bound by Alizarin Red-S. Adipogenic differentiation was evaluated by Sudan Black B stain; lipid droplets were photographed under light microscopy.

Induction of neuronal phenotype

Primary cultures of hMSC were chemically induced towards a neuronal phenotype (hMSC-n) according to the method of Woodbury et al. [12] with some modifications. Briefly, subconfluent cultures in 100 mm dishes were preinduced for 24 h in Neurobasal medium containing 1 mM β-mercaptoethanol (BME) and 10 ng/ml bFGF. The preinduction medium was then removed, and the cells were washed once with phosphate buffered saline (PBS). Successively, hMSC were shifted into Neurobasal medium containing 10% FCS, 10 mM BME for further 24 h.

Viability assay

Viable cells were determined in hMSC-n vs. control cells by Trypan blue dye exclusion test. Briefly, cells were cultured in 100 mm and were stained with Trypan blue dye for 1 min. Blue-positive and white-negative cells were counted in ten 20× fields, and the results were expressed as mean ± SE of viable and dead cells/field in three different experiments.

RT-PCR studies

Total RNA was isolated using Nucleospin®RNAII (Macherey-Nagel Duren, Germany) with DNAse treatment according to the manufacturer's instructions and the concentration determined spectrophotometrically with Nanodrop® ND-1000. First strand cDNA was synthesized using "TaqMan Reverse transcription Reagents" (Applied Biosystem Inc., Foster city, CA) with Reaction Buffer 1×; $MgCl_2$ 5.5 mM; dNTP's 2 mM; RNAse Inhibitor 1U; random hexamers 1.25 μM; MuLV 2U. In order to identify the presence of neuronal, osteogenic, chondrogenic and adipogenic markers, PCR was performed in 25 μl total volume using Mastermix AmpliTaq Gold (Applied Biosystem Inc., Foster city, CA) 1×, $MgCl_2$ 2 mM, forward and reverse primers 0.4 pmol/μl. Eppendorf Mastercycler Gradient (Eppendorf Amburg, Germany) was programmed as follows: 1 cycle at 95°C for 120 s, 30 cycles at 95°C for 45 s, 60°C for 45 s, and 45 s at 72°C. The primers (MWG biotech Germany) are reported in the table. The PCR products were analyzed on 2% or 3% agarose gels with ethidium bromide and visualized under UV light by Kodak Image Station 140 CF.

Gene product	Genbank accession number	Reference
Osteocalcin	BC033656	[19]
Bone sialoprotein	NM004967	[19]
Alkaline phosphatase	BC021289	[20]
PPARγ	BC006811	[21]
Type I collagen alpha 2 subunit	BC042586	[20]
Nestin	X65964	[22]
Necdin	AB007828	[22]
Neurofilament subunit L (NF-L)	X05608	[22]
Neurite outgrowth-promoting protein (NOPP)	X55110	[22]
Glypican 4 (GP4)	AF030186	[22]
Glial fibrillary acid protein (GFAP)	S40719	[22]

Immunocytochemistry

hMSC were cultured into four-chamber slides and induced to neuronal differentiation as described above. Successively, the cells were washed twice with PBS and fixed in 4% paraformaldehyde and 0.1% glutaraldehyde. hMSC were immunostained for nestin (mouse anti-nestin human antibody), choline acetyltransferase (ChAT, rabbit anti-choline acetyltransferase antibody), neuronal nuclei (NeuN, mouse anti-neuronal nuclei antibody), neurofilament M (NF-M, rabbit anti-neurofilament M C-terminal antibody). The cells were incubated with primary antibodies overnight at 4°C, incubated with secondary antibodies for 1 h followed by exposure to Vectastain ABC and AEC reagents (Vector Laboratories, Inc, Burlingame, CA, USA).

Electrophysiological studies

The electrophysiological behavior of hMSC and hMSC-n was analyzed by the whole-cell patch-clamp technique in voltage-clamp conditions. The cells were superfused at a rate of 1.8 ml min^{-1} with a control bath solution containing 150 mM NaCl, 5 mM KCl, 2.5 mM $CaCl_2$, 1 mM $MgCl_2$, 10 mM D-glucose and 10 mM HEPES. To block K^+ channels [23], we used a 20 mM-TEA bath solution containing 122.5 mM NaCl, 2 mM $CaCl_2$, 20 TEA-OH and 10 mM HEPES. To record Ca^{2+} currents, a TEA–Ca^{2+} bath solution (10 mM $CaCl_2$, 145 TEABr and 10 mM HEPES) was

used. 10 μM nifedipine and 100 μM Cd^{2+} (added as $CdSO_4$) were used to block respectively L-type Ca^{2+} channels and high voltage activated (HVA) but T-type Ca^{2+} channels. The patch pipettes filling solution contained 150 mM CsBr, 5 mM $MgCl_2$, 10 mM EGTA and 10 mM HEPES. pH was titrated to 7.4 with NaOH and to 7.2 with TEA-OH for bath and pipette solution, respectively. Patch electrodes were pulled using a micropipette vertical puller (Narishige PC-10) from borosilicate glass (GC 150-15; Clark). When filled, the resistance of the pipettes measured 2–3 MΩ. The patch pipette was connected to a micromanipulator (Narishige International USA) and an Axopatch 200B amplifier (Axon Instruments). Voltage-clamp protocol generation, data acquisition and analysis of data were as in Francini et al. [24]. Electrode capacitance was compensated before disrupting the patch. All the passive properties parameters were estimated as in Formigli et al. [25]. All experiments were performed at room temperature (20–23°C). The steady-state ionic current activation was evaluated by

$$I_a(V) = G_{max}(V - V_{rev})/\{1 + \exp[V_a - V/k_a]\} \quad (1)$$

and steady-state inactivation by

$$I_h(V) = I\{1 + \exp[-(V_h - V)/k - h]\} \quad (2)$$

where G_{max} is the maximal conductance for the I_a, V_{rev} is the apparent reversal potential, V_a and V_h are the potentials that elicit the half-maximal size, k_a and k_h are the steepness factors.

Quantitative real-time RT-PCR for human Telomerase Reverse Transcriptase (hTERT) and seladin-1 transcripts

The absolute quantification of hTERT mRNA (in hMSC and hMSC-n) and seladin-1 mRNA (in hMSC, hMSC exposed to 1 mM BME, 20 and 100 μM H_2O_2, 50 μM ascorbic acid, hMSC-n, hMSC-derived osteoblasts, human hippocampus, spinal cord, adrenal cortex, thyroid) was performed by real-time RT-PCR, based on TaqMan technologies, as described previously [26,27]. Because normalization to rRNA or to glyceraldehyde-3-phosphate-dehydrogenase, as well as to other "housekeeping" genes, has been clearly shown to be not accurate [28], the results were referred to microgram of total RNA. The experiments (n = 3) were run in triplicates.

Western blot analysis for seladin-1

The amount of seladin-1 protein in hMSC and in hMSC-n was determined by Western blot analysis, as described previously [27] using a rabbit polyclonal anti-seladin-1 antibody (1:2000) provided by Dr. Isabell Greeve [1].

Cholesterol measurement

The amount of cholesterol in hMSC and hMSC-n was determined by gas chromatography-mass spectrometry (GC-MS) using stigmasterol as internal standard. hMSC were harvested from plates in PBS with a rubber policeman, pelleted by centrifugation and frozen in liquid nitrogen for storage at –80°C. Cell pellets were homogenized in 20 mM Tris–HCl, pH 7.6, with three short pulses of a polytron homogenizer (Ultraturrax T8, IKA LABORTECHNIK, Germany). The protein concentration was determined in the cell lysate by the method of Bradford [29] using bovine serum albumin as reference standard. Aliquots corresponding to 5 μg of protein were used for cholesterol determination. After the addition of stigmasterol (1000 ng), sterols were saponified in 1.5 ml of freshly prepared 1 N NaOH in MeOH at 40°C for 60 min and successively extracted with 2 ml of *n*-hexane. After evaporation of the organic solvent, sterols were derivatized in 100 μl of *N*,*O*-bis(trimethylsilyl)-trifluoroacetamide (BSTFA) with 10% trimethyl-chlorosilane at 70°C for 30 min. Two microliters of the BSTFA solutions was automatically injected for analysis. A six-point calibration curve in the range 50–2000 ng of cholesterol with 1000 ng of stigmasterol as internal standard was used for cholesterol quantification. Each point was obtained by adding the appropriate quantities of cholesterol and internal standard and performing the same procedure of the samples. Stock solutions (1 μg/μl) of cholesterol and stigmasterol were prepared in ethanol. The peak area ratios (PAR) were calculated using the signals at 458 *m*/*z* and 484 *m*/*z* for cholesterol and stigmasterol, respectively. GC-MS analysis was conducted on a Hewlett-Packard GC-MS system composed of a 5890 series II gas-chromatograph equipped with a 5971A Mass Spectrometry Detector and a 7673A automatic injector. The GC column was a J&W DB1 (15 m × 0.25 mm × 0.25 μm), and the instrumental conditions were as follows: injector temperature: 250°C; temperature program of the GC column: 80 C × 1 min then 30°C/min to 240°C, then 5°C/min to 300°C, 300°C for 2 min. Injections were performed in the splitless mode with a purge off time of 1 min. SIM analyses were made acquiring the ions 458 *m*/*z*, 368 *m*/*z*, 353 *m*/*z* and 329 *m*/*z* for cholesterol and 484 *m*/*z* and 394 *m*/*z* for stigmasterol.

Statistical analysis

Data were expressed as mean ± SE or SD. Statistical differences were analyzed using one-way analysis of variance. Significance was adjusted for multiple comparisons of means using Bonferroni's approximation.

Results

Characterization of hMSC

hMSC were successfully culture-expanded. A morphologically homogeneous population of fibroblast-like cells with more than 90% confluence was seen after 14 days, and after the first passage, the cells grew exponentially, requiring weekly passages: primary culture cells (14 days) were trypsinized and replated, reaching a cellular expansion up to a 10^9–10^{10} factor in 5 months. The CFU-F assay was used as a surrogate assay for hMSC: the estimated Colony Forming Unit Efficiency of total nucleated cells was 50 ± 7 (mean ± SE)/10^6 cells.

Flow cytometry analysis was used to assess the purity of hMSC cultures, which appeared uniformly positive for CD29 (β_1 integrin), CD44 (receptor for hyaluronic acid), CD166

(activated leucocyte cell adhesion molecule-1, ALCAM-1), CD90 (Thy-1), CD73 (ecto-5′-nucleotidase), HLA-ABC and CD105 (type III TGFβ_{1-3} receptor or endoglin) (Fig. 1). HLA-DP QR was expressed in less than 2% of the population. There was no detectable contamination of hemopoietic cells: in fact, markers of the hemopoietic lineage, such as the lipopolysaccharide receptor CD14, CD34 and the leucocyte common antigen CD45, were not detectable (Fig. 1).

The expression of a panel of typical mesenchymal genes was examined in order to confirm the mesenchymal derivation of the primary cultures. hMSC expressed detectable levels of bone sialoprotein, osteocalcin, PPARγ, type I collagen and alkaline phosphatase transcripts (Fig 2A).

Osteogenic, adipogenic and chondrogenic differentiation of hMSC were readily inducible, further indicating that these cells were of mesenchymal derivation (Fig. 2B).

Neuronal differentiation of hMSC

Starting from the first hours of neuronal induction of hMSC (Fig. 3A) (see Materials and methods), the cells markedly changed their morphology under light microscopy, showing a neuronal-like phenotype (hMSC-n). Cytoplasm progressively retracted towards the nucleus and some neurite-like processes became apparent (Fig. 3B). 100% cell viability was documented after neuronal differentiation, thus excluding a toxic effect of BME (not shown).

The cells were assessed for the expression of neuronal-specific genes before and after neuronal induction by RT-PCR analysis. Undifferentiated hMSC showed transcripts only for nestin and GP4 (Fig 4A), two genes that are prevalently expressed by neuronal progenitor cells, whereas hMSC-n showed also transcripts for necdin and for the other neuronal-specific markers NF-L and NOPP [15], as shown in Fig. 4A. No amplified transcript for GFAP, a typical astrocyte marker [15], was detectable. Further characterization of differentiated neuronal cells was performed by immunocytochemistry (Fig. 4B). Most of the hMSC exhibited strong positive staining for nestin (Fig. 4Ba), whereas the positivity was markedly reduced in hMSC-n. The expression of NF-M, a neuronal-specific intermediate filament associated with neuritogenesis, neural process outgrowth and appearance of mature neuron morphology [30], was also tested. NF-M was highly expressed by hMSC-n (Fig. 4Bb) but was totally absent in hMSC. Positive staining for the established marker of motor neurons ChAT [31] was strongly detected in hMSC-n (Fig. 4Bc), whereas no signal was present in undifferentiated hMSC. Moreover, the expression of NeuN, the neuronal-

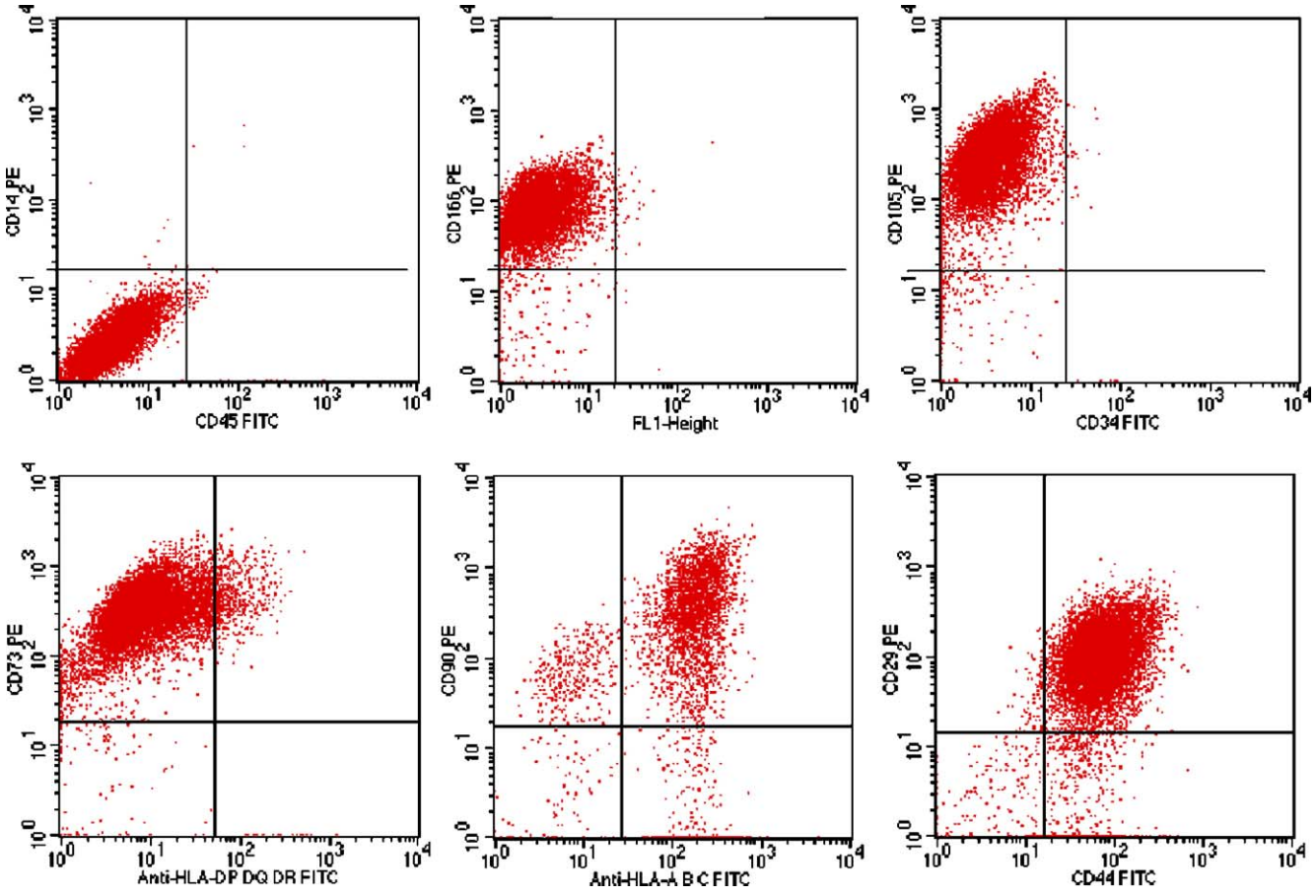

Fig. 1 – Flow cytometric analysis of surface adhesion molecules on hMSC. Cultures of hMSC were labeled with monoclonal antibodies specific for molecules indicated in each flow cytometric histogram: they are negative for CD45, CD14, CD34 and HLA-DP DQ DR; they are positive for CD105, CD166, CD90, CD73, CD29, CD44 and HLA-ABC.

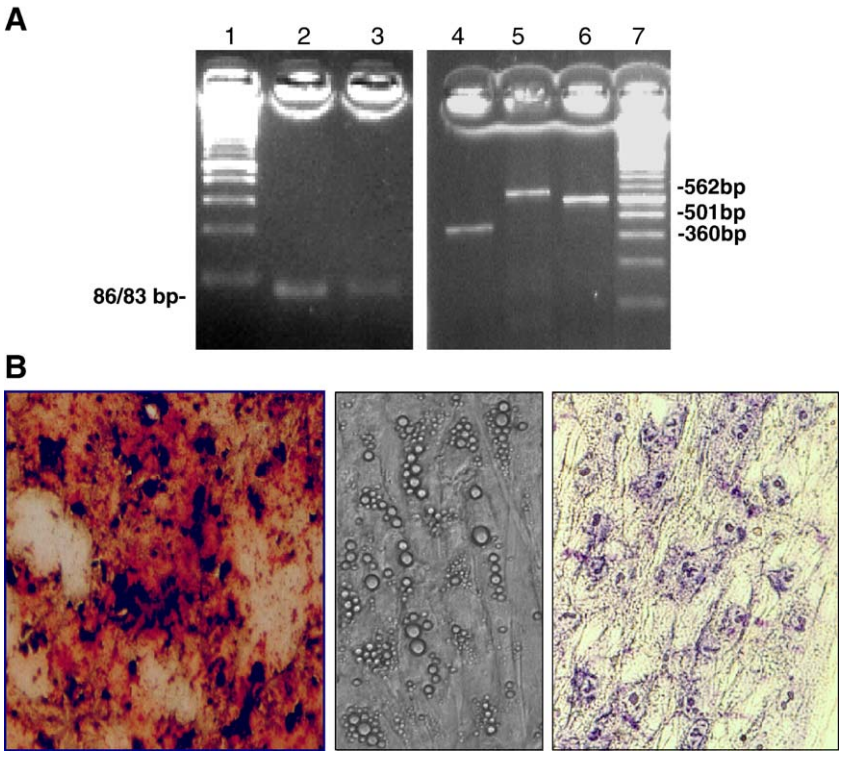

Fig. 2 – (A) Expression of typical mesenchymal genes in hMSC, as assessed by RT-PCR. Lanes 1 and 7, Molecular Weight Marker XIV (Roche-Hoffmann, Basel, Switzerland); 2, bone sialoprotein; 3, osteocalcin; 4, PPARγ; 5, type I collagen; 6, alkaline phosphatase. (B) Osteogenic (Alizarin Red S staining), adipogenic and chondrogenic differentiation (Toluidine Blue staining) of hMSC after 3 weeks in differentiation media.

specific marker of postmitotic cells [32], was tested. hMSC did not exhibit any positive immunostaining for NeuN, whereas hMSC-n showed an intense signal (Fig. 4Bd).

Electrophysiological studies

The cells were then assessed for the functional expression of specific ionic channels. All the hMSC investigated in control bath solution at a holding potential (HP) of –90 mV showed outward currents. Most of them showed a relatively slowly activating current (Fig. 5A) that occurred starting from –40 mV and slightly inactivated at positive potentials during 4.6-s-long pulses. Cell capacitance was 40 ± 2 pF. Mean current density was 19 ± 1.8 pA/pF at +50 mV. Current–voltage relation showed a change in steepness above +10 mV, suggesting the presence of two different kinds of outward currents (Fig. 5C, filled circles). To test whether the high voltage activated current was due to MaxIK channel activation, the other K^+ currents were blocked by setting the HP at –30 mV. In this condition, the outward current arose from 0 mV, it was fast activating and slightly inactivated at positive potentials (Fig. 5B). Mean current density was 15 ± 2.8 pA/pF at +50 mV.

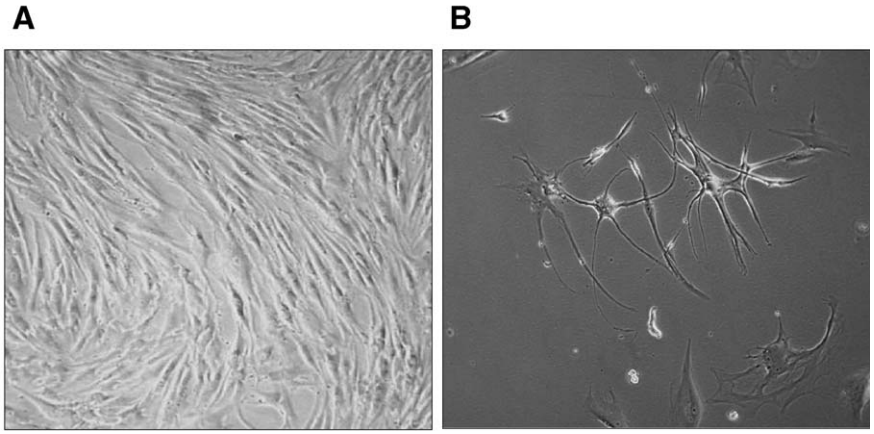

Fig. 3 – hMSC (A) and hMSC-n (B) shown by phase contrast inverted microscopy.

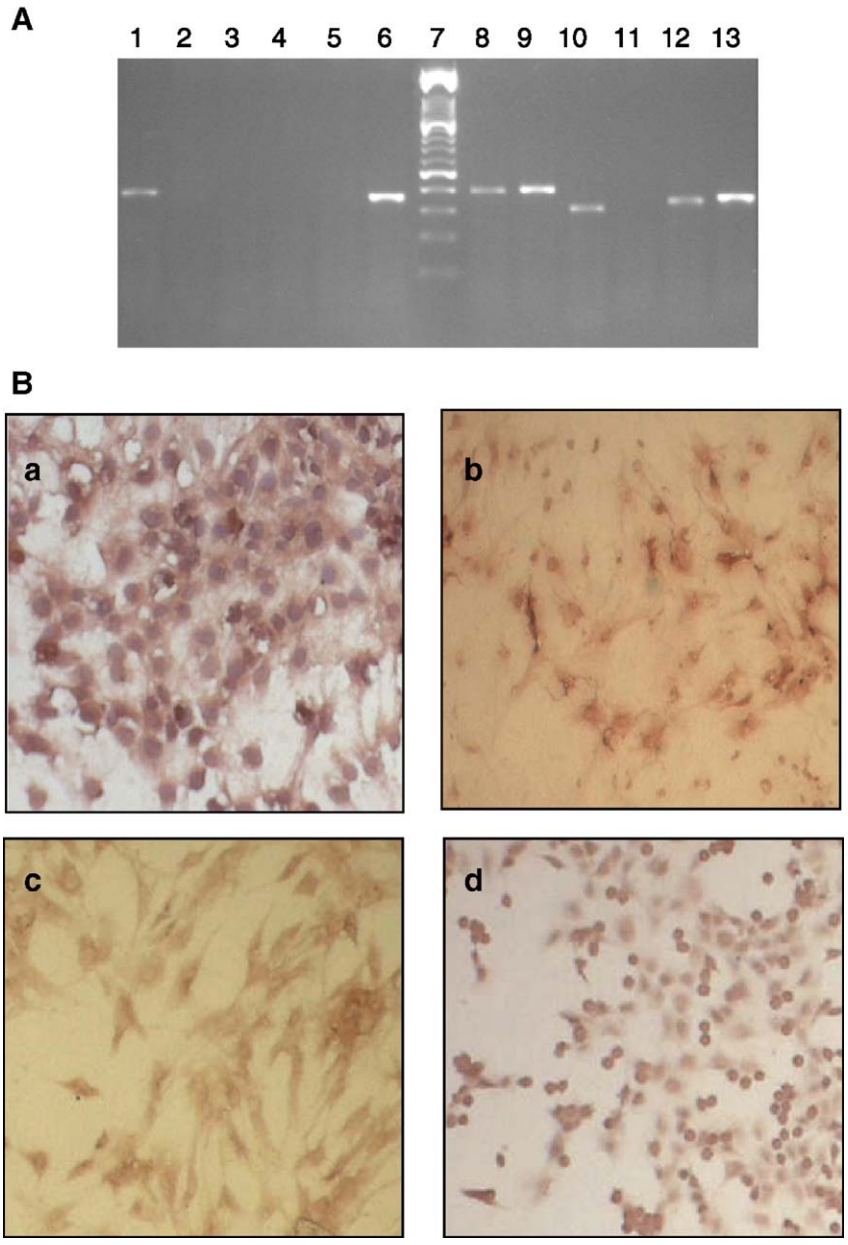

Fig. 4 – (A) Expression of neuronal markers in hMSC and in hMSC-n, as assessed by RT-PCR. Lanes 1 and 8, nestin; 2 and 9, necdin; 3 and 10, NF-L; 4 and 11, GFAP; 5 and 12, NOPP; 6 and 13, GP4; 7, Molecular Weight Marker XIV (Roche-Hoffmann). (B) Immunocytochemistry showing positivity for nestin in hMSC (a) and for NF-M (b), ChAT (c) and NeuN (d) in hMSC-n.

Activation of this current was associated with an increasing noise in the current recordings. *I–V* relation is showed in Fig 5C (filled triangles). The observed characteristics of such a current agree with MaxIK channel activation. Thus, outward current recorded with control bath solution at –90 mV HP was due to at least two kinds of K^+ channels roughly corresponding to I_s and I_r (MaxIK) described by Heubach et al. [23]. The *I–V* relation of I_s was evaluated by subtracting the data obtained at –30 mV from those at –90 mV HP (Fig. 5C, open circles). These currents were blocked by TEA–Ca^{2+} bath solution, indicating that they were K^+ currents. Na^+ and Ca^{2+} inward currents were absent in all the cells investigated.

hMSC-n showed drastic differences of currents time course. In control solution, inward transient currents preceded outward currents (Fig. 5D). To evaluate the involvement of functional Ca^{2+} channels, we used TEA–Ca^{2+} bath solution (Fig. 6A). An inward transient current was recorded from –50 mV with a peak at 80–100 ms. From –30 mV, it is followed by a slower decay suggesting the activation of HVA-type Ca^{2+} channels. Activation and inactivation Boltzmann curve of these two currents agree with T- and HVA-type of Ca^{2+} channels (Figs. 6C–E). This was confirmed by using Cd^{2+} and nifedipine since none of them affected T-type current (Fig. 6B). Instead, HVA-type was blocked by Cd^{2+} but not completely by nifedipine. Accordingly, HVA currents consist of the nifedipine-sensitive L-type and also other Ca^{2+} currents such as N, P, Q and R-types.

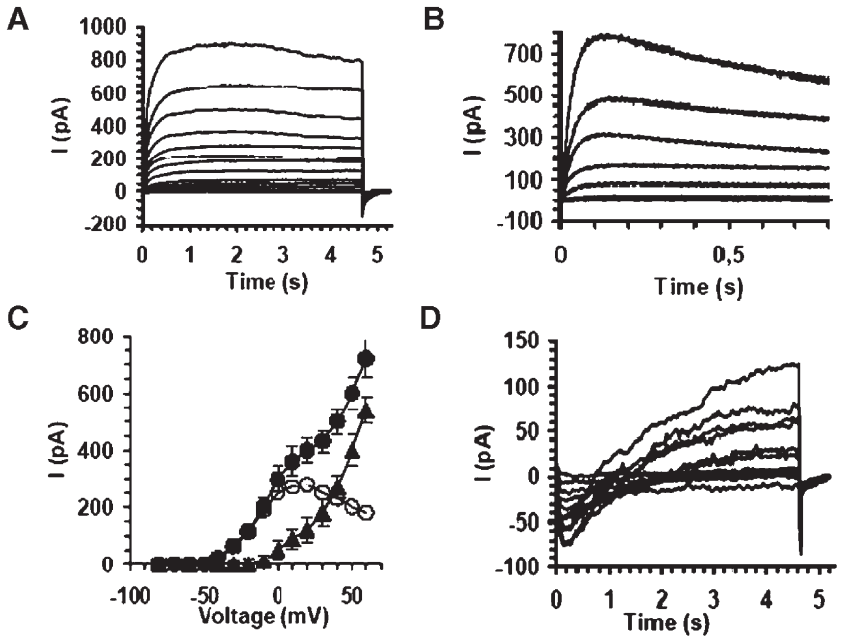

Fig. 5 – Ionic currents in hMSC and hMSC-n. Original current traces recorded in a typical hMSC in Control solution at a holding potential of –90 mV (A) and –30 mV (B); voltage steps from –80 to 60 mV in 10-mV increments. (C) Related *I–V* curves (filled circles, *n* = 9 cells) and –30 mV (filled triangles, *n* = 6 cells); open circles are data from the difference filled circles minus filled squares data. Inward currents precede outward currents in hMSC-n (D).

To assess the presence of inward Na^+ currents without the contamination of K^+ currents, we used 20 mM-TEA bath solution to block K^+ currents while the occurrence of T-type Ca^{2+} current was avoided by inactivating channels at –60 mV HP. In this experimental condition, we could record a fast inward transient current, with a time to peak at 0.5 ms and resolved in about 2 ms at –10 mV (Fig 6F). It activated from –50 mV, and its current–voltage relation showed a maximum at –10 mV (Fig. 6G). The current density at the peak was 18 pA/pF. The Boltzmann parameters values for activation were G_{max} = 12.7 pS, V_a = –25 mV, k_a = 7.4 and V_{rev} = 61 mV and for inactivation were V_h = –70; k_h = 7.4 mV (Figs. 6G, H). The divergence between half values was 45 mV. Since this current was not observed in TEA–Ca^{2+} bath solution that was Na^+-free and was blocked by TTX 1 μM, we can reasonably assess that it is a Na^+ current. Finally, being the time constant of inactivation 0.5 ms at –10 mV, all our data perfectly agree with the presence of Na^+ channels of neuronal type in these cells.

Expression and activity of seladin-1 in hMSC and in hMSC-n

The expression level of seladin-1 was evaluated by real-time RT-PCR and by Western blot analysis. The amount of seladin-1 transcript significantly decreased following neuronal differentiation of hMSC (Fig. 7); similarly, the level of seladin-1 protein also decreased in hMSC-n (Fig. 7). As an additional clue that in our experimental conditions hMSC were effectively differentiated into mature cells, we found a lower expression level of the catalytic subunit of telomerase, hTERT [33,34], in hMSC-n compared to undifferentiated cells (287 ± 21.8 vs. 8326 ± 732 ag/μg total RNA, mean ± SE, $p < 0.01$).

In order to clarify whether the reduction of seladin-1 expression might be related to the oxidative status of the cells, as shown by Wu et al. in immortalized fibroblasts, in which H_2O_2 increased seladin-1 expression [35], hMSC were exposed to H_2O_2 as well as to BME, which posseses anti-oxidant activity. 20 and 100 μM H_2O_2 (a sublethal concentration for hMSC) determined only a rapid and transient increase of seladin-1 expression after 6 h followed by a marked decline after 12 h. Exposure to 1 mM BME also determined an increase of seladin-1 expression after 6 h followed by a decrease after 12 h (Fig. 8). It has to be mentioned that MSC assume some neuronal characteristics already after a few hours of exposure to BME [12]. As an additional demonstration that the reduced level of expression of seladin-1 was associated to cell differentiation of hMSC, a significant decrease of the amount of transcript was observed when these cells were differentiated into hMSC-n using retinoic acid (52.9 ± 9%, hMSC-n, vs. 100 ± 3.8%, hMSC, mean ± SE, $p < 0.05$), as described and validated previously [15], instead of BME, or into osteoblasts (25.5 ± 2%, mean ± SE, $p < 0.05$). In the latter case, ascorbic acid, a known anti-oxidant agent, was among the factors used to induce cell differentiation, according to the literature [18]. However, short-term exposure (12 h) to 50 μM ascorbic acid did not change the amount of seladin-1 mRNA in hMSC (102.4 ± 3.5%, mean ± SE), compared to untreated cells.

As a further clue supporting the hypothesis that seladin-1 is a predominant product of stem cells, we also detected a high amount of seladin-1 mRNA in the human adult hippocampus and spinal cord, which have been shown to contain neural

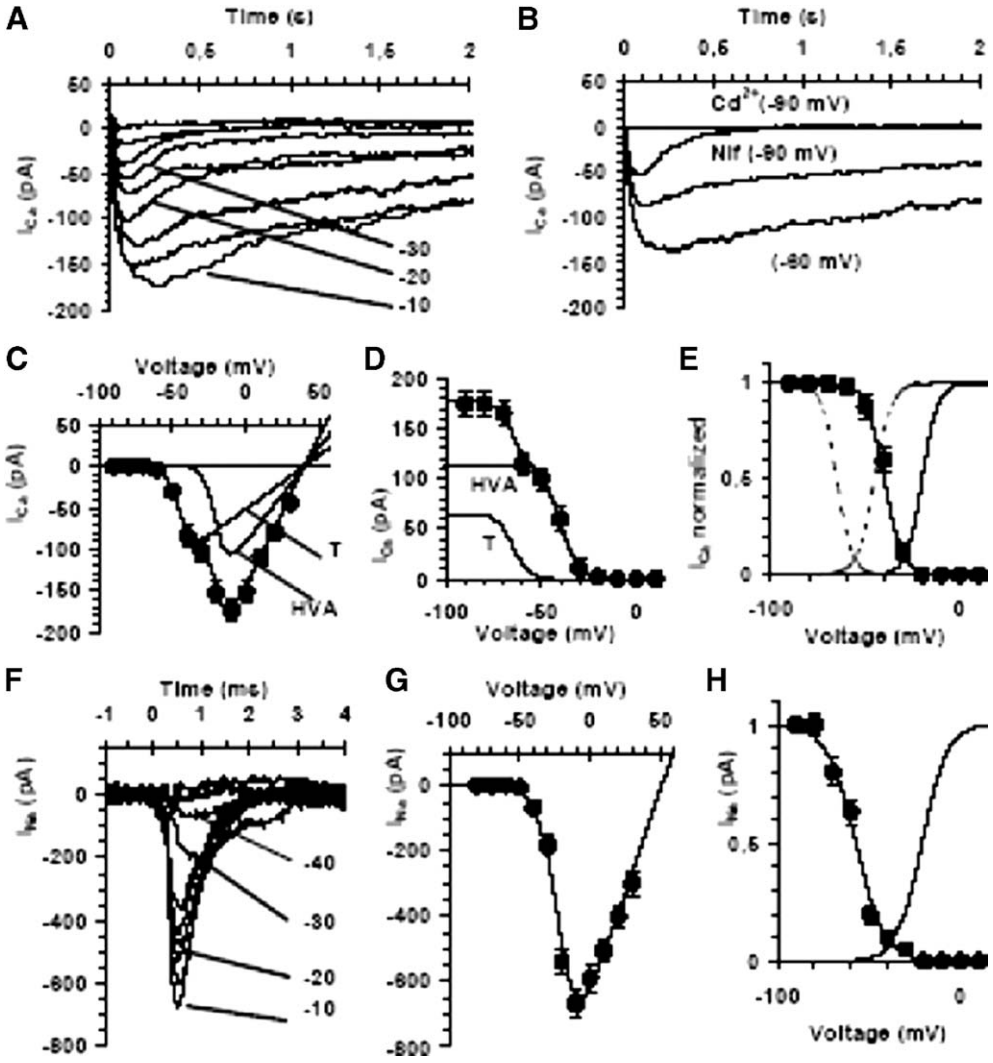

Fig. 6 – Inward Ca^{2+} and Na^{+} currents in hMSC-n. (A) Typical current traces recorded in TEA–Ca^{2+} bath solution from an HP at –90 mV; for clarity, only current traces from –60 to +20 mV are presented. The –30 mV traces clearly indicate the fast activating and inactivating T-type Ca^{2+} current followed by a slower inactivating one (HVA). (B) HVA currents recorded at HP of –60 mV or –90 mV with Nifedipine or Cd^{2+}. (C) *I–V* relation determined at the current peak ($n = 6$); superimpose continuous line to the data is the fit of the sum of two Boltzmann equations [Eq. (1)]; T and HVA lines are the related Boltzmann curves with $V_a = -45$ mV, $k_a = 4.4$ and $V_{rev} = 40$ mV and $V_a = -20$ mV, $k_a = 4.0$ and $V_{rev} = 40$ mV. (D) Inactivation *I–V* relation evaluated at test potential of –10 mV ($n = 5$): the best fit is obtained by a sum of two Boltzmann equations [Eq. (2)]; the related single Boltzmann fit is also presented to put in evidence the T- and HVA-type Ca^{2+} current inactivation. (E) Normalized *I–V* relation for activation and inactivation of T (dashed lines) and HVA-type (continuous line) Ca^{2+} currents from C and D; symbols are experimental data of HVA Ca^{2+} current evaluated at test potential of –10 mV from an HP –60 mV. (F) Inward Na^{+} currents (I_{Na}) recorded in 20-TEA bath solution at a holding potential of –60 mV. Representative current traces at voltage steps from –50 to +30 mV are shown; numbers related to some current traces indicate the pulse potential. (G) *I–V* relationship for I_{Na} peak ($n = 8$). Smooth curve is a Boltzmann curve from Eq. (1) with $V_a = -21$ mV, $k_a = 6.7$ and $E_{rev} = 51$ mV. (H) Normalized inactivation curve in 20-TEA bath solution determined by a test potential step to 0 mV following 1 s conditioning steps from –90 to 30 mV in 10-mV increments, HP at –60 mV; smooth curve superimposed on the data is a Boltzmann curve from Eq. (2) with $V_h = -57$ mV, $k_h = 7.5$. (The activation curve from G is depicted to show the overlapping window of potential where Na^{+} channels may simultaneously activate and are partially available to activate).

stem cells with neurogenic activity [8–10] (Table 1). The level of seladin-1 mRNA in these regions was rather close to the amount of transcript detected in the adrenal cortex, one of the tissues in which the highest levels of transcription had been detected [1]. In the thyroid gland, one of the organs in which low levels of seladin-1 mRNA had been observed [1], a markedly lower amount of transcript was detected (Table 1).

Finally, in order to test whether the reduced expression of seladin-1 in hMSC-n was paralleled by a decrease in cholesterol content, the amount of total cholesterol was determined

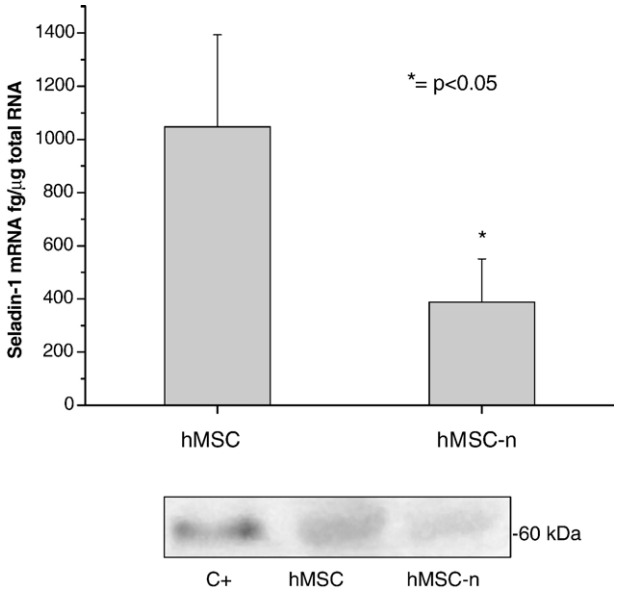

Fig. 7 – Amount of seladin-1 mRNA (top) and protein (bottom) in hMSC and in hMSC-n, determined by real-time RT-PCR and by Western blot analysis, respectively. C+, positive control, i.e. adrenal cortex [24].

by GC-MS in both hMSC and hMSC-n. Noticeably, a significant lower level of total cholesterol was measured in hMSC-n (155.1 ± 4.9 ng vs. 179.4 ± 1.3 ng, mean ± SD, $p < 0.01$).

Discussion

The discovery of the *seladin-1* gene and the finding that its expression is down-regulated in the brain areas affected in AD, the most prevalent form of late-life mental failure in humans [1], opened a new window for understanding the molecular events associated with neurodegeneration.

The aim of our study was to investigate on a possible explanation to the impaired seladin-1 expression in AD

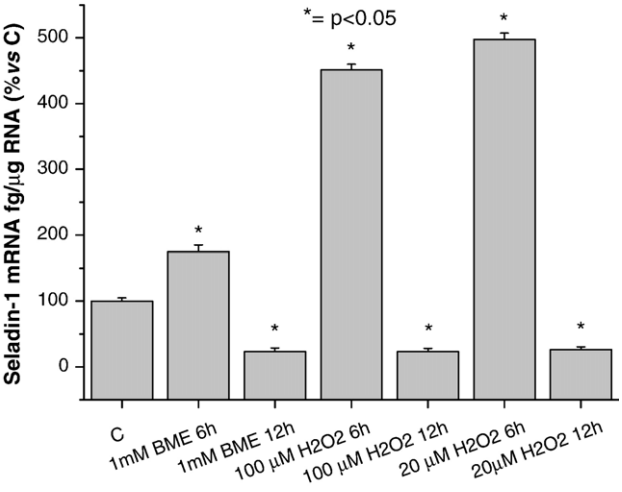

Fig. 8 – Effect of BME and H_2O_2 on seladin-1 mRNA in hMSC.

Table 1 – Amount of seladin-1 mRNA in different human adult tissues (mean ± SE)

Tissues	Seladin-1 mRNA
Hippocampus	5.16 ± 0.31 pg/μg total RNA
Spinal cord	6.97 ± 0.86 pg/μg total RNA
Adrenal cortex	8.82 ± 1.41 pg/μg total RNA
Thyroid	30.5 ± 3.34 fg/μg total RNA

vulnerable areas. The fact that some of these regions, namely the hippocampus and the subventricular zone, correspond to the areas which host stem cells with neurogenic potential and migratory activity in the adult brain [8], led us to hypothesize that seladin-1 might be a predominant product of multipotent cells. Therefore, we compared the amount of expression of the *seladin-1* gene in stem cells and in neuronal-like cells derived from them. Human MSC served as the multipotent cell model because they are much more easily obtainable than neuronal stem cells, and we rationalized that they might represent an acceptable alternative to the use of neuronal stem cells in our experimental setting. In fact, *in vitro* and *in vivo* neuronal differentiation of MSC into neurons has been demonstrated [12–15]. In addition, transplanted bone marrow cells have been localized in mouse [36] and human brain [37,38], suggesting a possible differentiation into neuronal cells. Recently, MSC have been injected intravenously, with encouraging results, into animals affected by experimental demyelination, ischemic stroke, amyotrophic lateral sclerosis and spinal cord injury [39] and also in humans affected by metachromatic leukodystrophy and Hurler syndrome, which present with severe neurological defects [40]. The functional/structural parallelism between neuronal stem cells and MSC has been underlined by the proposal to use terms like "neuropoiesis" to indicate the persistence of neurogenesis in the adult brain and "brain marrow" to describe the brain regions that contain cells supporting neurogenesis [41,42].

A fundamental point when working with stem cells is a thorough morphological and molecular characterization of these cells. In addition, each differentiation protocol has to be validated in order to exclude the presence of artifacts. Therefore, a substantial part of our work was dedicated to these aspects. hMSC were characterized by the analysis of the expression of representative genes and by the ability to differentiate into classical mesenchymal derivatives (i.e. fat, bone, cartilage). Neuronal differentiation was induced according to Woodbury et al. [12] and was validated by the demonstration of the expression of neuronal-specific markers, such as NF-L, NF-M, NOPP, ChAT, NeuN and necdin. In addition, thorough electrophysiological evaluation demonstrated that hMSC-n show Na^+ (I_{Na}) and Ca^{2+} (I_{Ca}) currents. These currents were consistently observed in all the cells and showed a larger current density compared to those reported for hMSC. Noticeably, the current time course and voltage dependence were different from those observed in hMSC [43], strongly supporting the idea that new types of functional ionic channels are expressed in hMSC-n. These channels were very likely of neuronal type, as suggested by additional experiments indicating that T- and HVA-Ca^{2+} channels of neuronal phenotype were expressed. Notably, these Ca^{2+} currents are those reported in neurons [44,45], whereas cardiac and

skeletal muscle express T and L-type channels with different properties [46,47]. With regard to the Na^+ current, Boltzmann parameters were also consistent with those found in differentiated neurons [48,49] and differed from those observed in cardiac and skeletal muscle cells [50].

The amount of both seladin-1 mRNA and protein markedly decreased in hMSC-n compared to hMSC. Accordingly, the expression level of the catalytic subunit of telomerase hTERT dramatically decreased after cell differentiation. This finding is in agreement with the fact that telomerase is highly expressed in germ and stem cells, including MSC, and its expression has been related to the differentiating ability [33]. Conversely, low levels of expression are detected in quiescent or terminally differentiated cells [34]. In agreement with the reduced amount of expression of seladin-1, the content of total cholesterol was found to be significantly decreased in hMSC-n.

Because a previous study reported that sublethal doses of H_2O_2 were able to increase seladin-1 expression in immortalized fibroblasts (yet the maximum effect was observed after 12 h of treatment and was markedly decreased after 24 h) [35], we wondered whether the oxidative status of hMSC might influence seladin-1 expression. We found that H_2O_2 determined only a rapid (after 6 h) and transient increase of seladin-1 transcript followed by a marked decrease after 12 h. Similar results were obtained upon exposure to BME, which was used in our experimental design to induce neuronal differentiation and which possesses anti-oxidant activity. The fact that after a few hours of exposure to BME MSC already assume some neuronal characteristics [12] supports the hypothesis that the decrease of seladin-1 expression is associated to cell differentiation. Furthermore, we have shown that also upon induction of neuronal differentiation using another differentiating factor (i.e. retinoic acid), instead of BME, the amount of seladin-1 transcript was significantly reduced. As a further clue that the decreased expression of seladin-1 is linked to the differentiation process, we obtained a significant reduction of the amount of mRNA also following differentiation of hMSC into osteoblasts.

The results here reported represent the first demonstration that the *seladin-1* gene is a predominant product of stem cells. On the basis of these observations, it could be suggested that the defective seladin-1 expression detected in AD vulnerable brain regions may be linked to an impaired neuronal stem cell compartment that could be a potential risk factor to develop this disease. With regard to this point, it is worth mentioning that, according to the findings of Greeve et al. [1], we detected high levels of seladin-1 transcript in the adult hippocampus, a well-known neurogenic brain region [8], and which is one of the areas affected in AD. Similarly, a high amount of seladin-1 mRNA was found in the spinal cord, in which stem cells with neurogenic properties have been recently described [9,10]. Alternatively, our findings might indicate a modification of the neurogenic properties of the adult brain as a consequence of neuronal damage and therefore of AD itself. In agreement with the latter hypothesis, decreased proliferation of neuronal precursors has been observed in animal models of AD, and it has been linked to β-amyloid toxicity [51]. In any case, the decrease of seladin-1 expression might be viewed as a marker of neuronal damage in AD [1].

Finally, although the data presented in this study should be further supported by additional experimental strategies involving different stem cell models, in view of our results, it is tempting to speculate that reinforced seladin-1 expression might be an additional point to be raised in favor of a stem-cell-based therapy in AD, once several critical issues (i.e. the ideal stem cells source for transplantation, the route of administration, the achievement of an appropriate and long-lasting integration of transplanted stem cells into the host tissue) will be solved [39].

Acknowledgments

This study was partially supported by grants from Regione Toscana (TRESOR project, principal investigator Prof. Mario Serio) and from Ente Cassa di Risparmio di Firenze.

REFERENCES

[1] I. Greeve, I. Hermans-Borgmeyer, C. Brellinger, D. Kasper, T. Gomez-Isla, C. Behl, B. Levkau, R.M. Nitsch, The human DIMINUTO/DWARF1 homolog seladin-1 confers resistance to Alzheimer's disease-associated neurodegeneration and oxidative stress, J. Neurosci. 20 (2000) 7345–7352.
[2] S. Benvenuti, P. Luciani, G.B. Vannelli, S. Gelmini, E. Franceschi, M. Serio, A. Peri, Estrogen and SERMs exert neuroprotective effects and stimulate the expression of seladin-1, a recently discovered anti-apoptotic gene, in human neuroblast long-term cell cultures, J. Clin. Endocrinol. Metab. 90 (2005) 1775–1782.
[3] H.R. Waterham, J. Koster, G.J. Romeijn, R.C.M. Hennekam, P. Vreken, H.C. Andersson, D.R. FitzPatrick, R.I. Kelley, R.J.A. Wanders, Mutations in the 3beta-hydroxysterol Delta24-reductase gene cause desmosterolosis, an autosomal recessive disorder of cholesterol biosynthesis, Am. J. Hum. Genet. 69 (2001) 685–694.
[4] N. Arispe, M. Doh, Plasma membrane cholesterol controls the cytotoxicity of Alzheimer's disease AbetaP (1–40) and (1–42) peptides, FASEB J. 16 (2002) 1526–1536.
[5] T.C. McMorris, Recent developments in the field of plant steroid hormones, Lipids 32 (1997) 1303–1308.
[6] G.J. Bishop, T. Nomura, T. Yokota, K. Harrison, T. Noguchi, S. Fujioka, S. Takatsuto, J.D. Jones, Y. Kamiya, The tomato DWARF enzyme catalyses C-6 oxidation in brassinosteroid biosynthesis, Proc. Natl. Acad. Sci. U. S. A. 96 (1999) 1761–1766.
[7] D.J. Selkoe, Alzheimer's disease: genes, proteins, and therapy, Physiol. Rev. 81 (2001) 741–776.
[8] D.C. Lie, H. Song, S.A. Colamarino, G.L. Ming, F.H. Gage, Neurogenesis in the adult brain: new strategies for central nervous system diseases, Annu. Rev. Pharmacol. Toxicol. 44 (2004) 399–421.
[9] Y. Ke, L. Chi, R. Xu, C. Luo, D. Gozal, R. Liu, Early response of endogenous adult neural progenitor cells to acute spinal cord injury in mice, Stem Cells 24 (2006) 34–43.
[10] A.I. Danilov, R. Covacu, M.C. Moe, I.A. Langmoen, C.B. Johansson, T. Olsson, L. Brundin, Neurogenesis in the adult spinal cord in an experimental model of multiple sclerosis, Eur. J. Neurosci. 23 (2006) 394–400.
[11] S. Temple, The development of neural stem cells, Nature 414 (2001) 112–117.
[12] D. Woodbury, E.J. Schwarz, D.J. Prockop, I.B. Black, Adult rat

and human bone marrow stromal cells differentiate into neurons, J. Neurosci. Res. 61 (2000) 364–370.
[13] D. Woodbury, K. Reynolds, I.B. Black, Adult bone marrow stromal stem cells express germline, ectodermal, endodermal and mesodermal genes prior to neurogenesis, J. Neurosci. Res. 69 (2002) 908–917.
[14] Y. Jiang, B.N. Jahagirdar, R.L. Reinhardt, R.E. Schwartz, C.D. Keene, X.R. Ortiz-Gonzalez, M. Reyes, T. Lenvik, T. Lund, M. Blackstad, J. Du, S. Aldrich, A. Lisberg, W.C. Low, D.A. Largaespada, C.M. Verfaillie, Pluripotency of mesenchymal stem cells derived from adult bone marrow, Nature 418 (2002) 41–49.
[15] J.R. Sanchez-Ramos, Neural cells derived from adult bone marrow and umbilical cord blood, J. Neurosci. Res. 69 (2002) 880–893.
[16] H. Castro-Malaspina, Characterization of human bone marrow fibroblast colony-forming cells (CFU-F) and their progeny, Blood 56 (1980) 289–301.
[17] A.J. Friedenstein, Precursor cells of mechanocytes, Int. Rev. Cytol. 47 (1976) 327–359.
[18] M.F. Pittenger, A.M. Mackay, S.C. Beck, R.K. Jaiswal, R. Douglas, J.D. Mosca, M.A. Moorman, D.W. Simonetti, S. Craig, D.R. Marshak, Multilineage potential of adult human mesenchymal stem cells, Science 284 (1999) 143–147.
[19] H.R. Haase, S. Ivanovski, M.J. Waters, P.M. Bartold, Growth hormone regulates osteogenic marker mRNA expression in human periodontal fibroblasts and alveolar bone-derived cells, J. Periodontal. Res. 38 (2003) 366–374.
[20] N. Ohara, Y. Hayashi, S. Yamada, S.K. Kim, T. Matsunaga, K. Yanagiguchi, T. Ikeda, Early gene expression analyzed by cDNA microarray and RT-PCR in osteoblasts cultured with watersoluble and low-molecular chitooligosaccharide, Biomaterials 25 (2004) 1749–1754.
[21] T. Kubota, K. Koshizuka, E.A. Williamson, H. Asou, J.W. Said, S. Holden, I. Miyoshi, H.P. Koeffler, Ligand for peroxisome proliferator-activated receptor gamma (troglitazone) has potent antitumor effects against human prostate cancer both in vitro and in vivo, Cancer Res. 58 (1998) 3344–3352.
[22] J.R. Sanchez-Ramos, S. Song, S.G. Kamath, T. Zigova, A. Willing, F. Cardozo-Pelaez, T. Stedeford, M. Chopp, P.R. Sanberg, Expression of neural markers in human umbilical cord blood, Exp. Neurol. 171 (2001) 109–115.
[23] J.F. Heubach, E.M. Graf, J. Leutheuser, M. Bock, B. Balana, I. Zahanich, T. Christ, S. Boxberger, E. Wettwer, U. Ravens, Electrophysiological properties of human mesenchymal stem cells, J. Physiol. 554 (2004) 659–672.
[24] F. Francini, C. Bencini, C. Piperio, R. Squecco, Separation of charge movement components in mammalian skeletal muscle fibres, J. Physiol. 537 (2001) 45–56.
[25] L. Formigli, E. Meacci, C. Sassoli, F. Chellini, R. Giannini, F. Quercioli, B. Tiribilli, R. Squecco, P. Bruni, F. Francini, S. Zecchi-Orlandini, Sphingosine 1-phosphate induces cytoskeletal reorganization in C2C12 myoblasts: physiological relevance for stress fibres in the modulation of ion current through stretch-activated channels, J. Cell Sci. 118 (2005) 1161–1171.
[26] T. Yajima, A. Yagihashi, H. Kameshima, D. Furuya, D. Kobayashi, K. Hirata, N. Watanabe, Establishment of quantitative reverse transcription-polymerase chain reaction assays for human telomerase-associated genes, Clin. Chim. Acta 290 (2000) 117–127.
[27] P. Luciani, P. Ferruzzi, G. Arnaldi, C. Crescioli, S. Benvenuti, A. Valeri, I. Greeve, M. Serio, M. Mannelli, A. Peri, Expression of the novel adrenocorticotropin-responsive gene selective Alzheimer's disease indicator-1 in the normal adrenal cortex and in adrenocortical adenomas and carcinomas, J. Clin. Endocrinol. Metab. 89 (2004) 1332–1339.
[28] S.A Bustin, Quantification of mRNA using real-time reverse transcription PCR (RT-PCR): trends and problems, J. Mol. Endocrinol. 29 (2002) 23–39.
[29] M.M. Bradford, A rapid sensitive method for the quantitation of microgram quantities of protein utilizing the principle of protein-dye binding, Anal. Biochem. 72 (1976) 248–254.
[30] M.J. Carden, J.Q. Trojanowski, W.W. Schlaepfter, V.M. Lee, Two-stage expression of neurofilament polypeptides during rat neurogenesis with early establishment of adult phosphorylation patterns, Neuroscience 7 (1987) 3489–3504.
[31] P. Tirassa, V. Triaca, T. Amendola, M. Fiore, L. Aloe, EGF and NGF injected into the brain of old mice enhance BDNF synthesis and increase the number of Ki67 and CHAT-positive cells in the subventricular zone, J. Neurosci. Res. 72 (2003) 557–564.
[32] H.B. Sarnat, D. Nochlin, D.E. Born, Neuronal nuclear antigen (NeuN): a marker of neuronal maturation in early human fetal nervous system, Brain Res. 20 (1998) 88–94.
[33] L. Liu, C.M. DiGirolamo, P.A. Navarro, M.A. Blasco, D.L. Keefe, Telomerase deficiency impairs differentiation of mesenchymal stem cells, Exp. Cell Res. 294 (2004) 1–8.
[34] J. Feng, W.D. Funk, S.-S. Wang, S.L. Weinrich, A.A. Avilion, C.P. Chiu, R.R. Adams, E. Chang, R.C. Allsopp, J. Yu, The RNA component of human telomerase, Science 269 (1995) 1236–1241.
[35] C. Wu, I. Miloslavskaya, S. Demontis, R. Maestro, K. Galaktionov, Regulation of cellular response to oncogenic and oxidative stress by Seladin-1, Nature 432 (2004) 640–645.
[36] E. Mezey, K.J. Chandross, G. Harta, Turning blood into brain: cells bearing neuronal antigens generated in vivo from bone marrow, Science 290 (2000) 1779–1782.
[37] E. Mezey, S. Key, G. Vogelsang, I. Szalayova, G.D. Lange, B. Crain, Transplanted bone marrow generates new neurons in human brain, Proc. Natl. Acad. Sci. 100 (2003) 1364–1369.
[38] J.M. Weimann, C.A. Charlton, T.R. Brazelton, R.C. Hackman, H.M. Blau, Contribution of transplanted bone marrow cells to Purkinje neurons in human adult brains, Proc. Natl. Acad. Sci. 100 (2003) 2088–2093.
[39] S. Pluchino, L. Zanotti, M. Deleidi, G. Martino, Neural stem cells and their use as therapeutic tool in neurological disorders, Brain Res. Rev. 48 (2005) 211–219.
[40] O.N. Koc, J. Day, M. Nieder, S.L. Gerson, H.M. Lazarus, W. Krivit, Allogeneic mesenchymal stem cell infusion for treatment of metachromatic leukodystrophy (MLD) and Hurler syndrome (MPS-ICH), Bone Marrow Transplant. 30 (2002) 215–222.
[41] D.A. Steindler, T. Kadrie, H. Fillmore, L.B. Thomas, The subependymal zone: "brain marrow", Prog. Brain Res. 108 (1996) 349–363.
[42] B. Scheffer, M. Horn, I. Blumcke, E.D. Laywell, D. Coomes, V.G. Kukekov, D.A. Steindler, Marrow-mindedness: a perspective on neuropoiesis, Trends Neurosci. 22 (1999) 348–357.
[43] G. Li, S. Haiying, X. Deng, C.P. Lau, Characterization of ionic currents in human mesenchymal stem cells from bone marrow, Stem Cells 23 (2005) 371–382.
[44] S.M. Todorovic, V. Jevtovic-Todorovic, S. Mennerick, E. Perez-Reyes, C.F. Zorumski, Ca(v)3.2 channel is a molecular substrate for inhibition of T-type calcium currents in rat sensory neurons by nitrous oxide, Mol. Pharmacol. 60 (2001) 603–610.
[45] N. Joux, V. Chevaleyre, G. Alonso, L. Boissin-Agasse, F.C. Moos, M.G. Desarmenien, N. Hussy, High voltage-activated $Ca2^{+}$ currents in rat supraoptic neurones: biophysical properties and expression of the various channel alpha1 subunits, J. Neuroendocrinol. 13 (2001) 638–649.
[46] K.G. Beam, C.M. Knudson, Calcium currents in embryonic and neonatal mammalian skeletal muscle, J. Gen. Physiol. 91 (1988) 781–798.
[47] C. Bencini, R. Squecco, C. Piperio, L. Formigli, E. Meacci,

D. Nosi, B. Tiribilli, M. Vassalli, F. Quercioli, P. Bruni, S. Zecchi Orlandini, F. Francini, Effects of sphingosine 1-phosphate on excitation–contraction coupling in mammalian skeletal muscle, J. Muscle Res. Cell. Motil. 24 (2003) 539–554.
[48] N. Yoshimura, W.C. De Groat, Characterization of voltage-sensitive Na+ and K+ currents recorded from acutely dissociated pelvic ganglion neurons of the adult rat, J. Neurophysiol. 76 (1996) 2508–2521.
[49] M. Albrieux, J.C. Platel, A. Dupuis, M. Villaz, W.J. Moody, Early expression of sodium channel transcripts and sodium current by Cajal-Retzius cells in the preplate of the embryonic mouse neocortex, J. Neurosci. 24 (2004) 1719–1725.
[50] T. Zimmer, C. Bollensdorff, V. Haufe, E. Birch-Hirschfeld, K. Benndorf, Mouse heart Na+ channels: primary structure and function of two isoforms and alternatively spliced variants, Am. J. Physiol.: Heart Circ. Physiol. 282 (2002) 1007–1017.
[51] N.J. Haughey, A. Nath, S.L. Chan, A.C. Borchard, M.S. Rao, M.P. Mattson, Disruption of neurogenesis by β-peptide, and perturbed neural progenitor cell homeostasis, in models of Alzheimer's disease, J. Neurochem. 83 (2002) 1509–1524.